IJCRT.ORG ISSN : 2320-2882

INTERNATIONAL JOURNAL OF CREATIVE RESEARCH THOUGHTS (IJCRT)

An International Open Access, Peer-reviewed, Refereed Journal

EXPERIMENTALLY INVESTIGATION OF NUSSELT NUMBER AND FRICTION FACTOR OF V-SHAPE ARTIFICIAL ROUGHNESS IN SOLAR AIR HEATERS

Sachin Baraskar[1], Santosh Kumar Rai[2]

[1]PhD scholar, [2]Research Director

[1]Department of Mechanical Engineering,

[1] Sri Satya Sai University of Technology and Medical Sciences, Sehore, M.P., India-466001

Abstract: The phenomenon of improving the heat transfer coefficient within a solar air heater duct through the incorporation of artificial roughness is a widely recognized concept in the field. The present investigation conducts an experimental examination that specifically focuses on the attributes of heat transfer and friction factor in a rectangular duct that has been deliberately roughened by the addition of repeated v-shape ribs. These ribs are strategically positioned on one of the wide walls of the duct, with variations including ribs with gaps and without gaps. The orientation of these ribs is set at a 60° angle with respect to the flow direction, with the primary objective being the enhancement of heat transfer efficiency. The duct being studied features an aspect ratio (W/H) of 8, a relative roughness pitch (p/e) of 10, a relative roughness height (e/Dh) of 0.030, and an angle of attack of 600. Through a comprehensive comparison between the heat transfer and friction characteristics of the roughened duct and a smooth duct operating under similar flow conditions, valuable insights can be gleaned regarding the impact of surface roughness on overall performance metrics. Particularly, a detailed analysis has been conducted to examine the influence of introducing a gap within the structure of the v-shaped ribs, encompassing a range of flow Reynolds numbers from 5387 to 13211. The results indicate that the presence of a gap within the rib configuration leads to a substantial improvement in both the Nusselt number and friction factor, with enhancements reaching 2.57 and 2.85 times, respectively, in comparison to the performance of the smooth duct arrangement. This analytical exploration provides a deeper understanding of the complex interactions between geometric features and flow properties in roughened ducts, thereby offering practical implications for optimizing heat transfer efficiency in solar air heating systems.

Keywords: Solar air heater; Heat transfer; Friction; Roughness; Reynolds Number

I.INTRODUCTION

The thermal efficiency of solar air heaters is frequently documented to be below standard because of their inherently restricted heat transfer capacity between the absorber plate and the air flowing through the duct. In order to make solar air heaters financially viable, it is crucial to elevate their thermal efficiency by increasing the heat transfer coefficient. The enhancement of a higher heat transfer coefficient requires the disturbance of the laminar sub-layer that forms near the absorber plate and the introduction of turbulence at the heat-transferring surface through the inclusion of artificial roughness. However, the incorporation of artificial roughness brings about increased frictional losses, leading to a substantial power requirement for fluid flow within the duct. Thus, it is of utmost importance to ensure that turbulence is induced only in the immediate proximity of the heat-transferring surface to disrupt the viscous sub-layer for enhancing heat transfer, while minimizing disruption to the core flow to prevent the rise in friction losses. This particular goal can be achieved by maintaining the height of the roughness elements significantly smaller than the dimensions of the duct. Furthermore, it is essential to carefully design the artificial roughness elements to promote turbulence generation while simultaneously mitigating the adverse effects of heightened frictional losses. The strategic placement of these roughness elements can play a pivotal role in optimizing heat transfer efficiency in solar air heaters, thereby making them more economically viable and environmentally friendly in the long run.

Various researchers have engaged in extensive investigations into a wide array of roughness geometries and their respective configurations aimed at enhancing heat transfer from surfaces involved in various heat transfer processes. As detailed by Han et al. [1], the scholars expound on a solar air heater that consists of an enclosure featuring a front-facing wall that is transparent or translucent towards the sun, a rear wall, and side walls positioned between the front and rear structures. Moreover,

the heater incorporates an inlet section facilitating the introduction of air, an outlet section from which solar-heated air is discharged, and a heating element located between the rear and front walls, traversed by the incoming air. This heating element is characterized by a multitude of three-dimensional, multi-directionally sloping protrusions crafted from a thermally insulating material. Zvulun et al. [2] direct their focus towards the global advancements witnessed in various facets of solar air heating systems since 1877, providing insights into some innovative patents related to Solar Air Heaters (SAHs). Abhishek et al. [3] have introduced a solar air heater featuring a support structure and a cylinder body affixed at the upper extremity of the support, with a series of through holes present on the lower surface of the cylinder body. Wu et al. [4] have meticulously designed, constructed, and assessed the performance of a solar air heater operating in the forced convection mode within the climatic conditions of Allahabad. This device, aimed at harnessing solar energy, emerges as a straightforward yet effective tool. Durgesh et al. [5] have unveiled the findings of a comprehensive evaluation concerning the environmental impacts arising from the deployment of such devices for preheating ventilation air. Additionally, calculations were conducted to estimate the potential annual energy savings achievable for typical residences, along with the prospective reduction in greenhouse gas (GHG) emissions. In a similar vein, Miroslaw et al. [6] the heat transfer and friction characteristics of artificially roughened solar air heaters with different roughness geometries have been reviewed in order to compare the performance of solar air heater having different types of roughness geometry. Vijay et.al [7] Experimental research has been conducted on solar air heaters equipped with box-type absorbers and heat storage units, revealing that the energy output of solar air heaters with heat storage is greater than that of those without such units. The study by W. Smolec et al. [8] delves into numerical simulations of thermal and aerodynamic processes within a solar air heater featuring a light-absorbing L-shaped fin. Through computational fluid dynamics (CFD) analysis, the impact of design factors such as the spacing between fins and technological variables like the Reynolds number on heat transfer and flow dynamics was elucidated. Dmitry et al. [9] define a solar air heater as having a transparent or translucent front panel with multiple flow passages, facilitating air movement from the inlet to the outlet through different channels. Arndt et al. [10, 11] have proposed a system aimed at continuously heating air using solar energy to a specific temperature for various domestic applications, including drying systems and indoor heating. Dibirov et al. [12] have conducted an economic assessment of solar air heaters enhanced with artificial roughness, specifically utilizing v-shaped structures to optimize life cycle savings from solar energy. R. Bahuguna et al. conducted further investigations on the efficiency and performance of these solar air heaters, contributing valuable insights to the field of renewable energy utilization. The integration of heat storage units in solar air heaters presents a promising avenue for enhancing energy delivery and overall system efficiency, especially in applications requiring consistent temperature control. Computational modeling techniques offer a valuable tool for studying the intricate thermal and aerodynamic processes within solar air heaters, enabling researchers to optimize design parameters and enhance performance. The utilization of transparent or translucent materials in the front panel of solar air heaters facilitates efficient heat absorption and transfer, contributing to improved overall system efficiency. Proposed systems for round-the-clock air heating using solar energy demonstrate the potential for sustainable and cost-effective heating solutions in various practical scenarios. Economic analyses of solar air heaters with innovative features provide valuable insights into the long-term cost-effectiveness and sustainability of such systems, guiding future research and development efforts in the field.

In consideration of the aforementioned points, it is possible to assert that discrete inclined or V-shaped rib arrangement demonstrates superior performance when compared to a continuous rib arrangement. Nevertheless, up to this point, there has been a lack of research conducted to analyze the impact of the gap width between the rib elements in forming the discrete rib pattern. Consequently, the current study was initiated to investigate the influence of the gap within the V-shape rib structure to create a discrete rib configuration. Within the scope of the ongoing research, an experimental exploration focusing on the efficiency of solar air heater ducts has been conducted. These ducts feature an absorber plate with artificial roughness in the form of V-shape ribs, with and without a gap. The range of flow Reynolds numbers considered in the experimentation varied from 3000 to 15,000. Through the assessment of the variations in Nusselt number and friction factor, in relation to roughness parameters such as gap position, the thermo-hydraulic performance of the system has been thoroughly analyzed. This evaluation serves to determine the advantages offered by the selected roughness geometry in enhancing the overall performance of the system.

II.EXPERIMENTAL SETUP

The experimental setup depicted in Figure 1 illustrates the schematic diagram showcasing the test section. The setup encompasses various components within the flow system, such as an entry section, a test section, an exit section, a flow meter, and a centrifugal blower. The dimensions of the duct's inner cross-section measure 2042 mm x 200 mm x 20 mm, constructed using wooden panels with a thickness of 25 mm. Specifically, the test section is 1500 mm in length, equivalent to 33.75 times the hydraulic diameter. The entry and exit sections have lengths of 192 mm (7.2 times the hydraulic diameter) and 350 mm (12 times the hydraulic diameter) respectively. The decision to opt for a short entrance length (L/Dh=7.2) was based on the premise that a roughened duct can achieve thermally fully developed flow within a short length of 2-3 hydraulic diameters. ASHRAE standard 93-77 stipulates that for the turbulent flow regime, the recommended entry and exit lengths are 5 times the square root of the hydraulic diameter (√WH) and 2.5 times the square root of the hydraulic diameter (√WH) respectively.

Upon reaching the exit section, particularly after 116 mm, three equally spaced baffles occupy a length of 87 mm. These baffles are strategically positioned to aid in mixing the hot air exiting the solar air duct, ensuring a uniform temperature of air (bulk mean temperature) at the outlet. An electric heater, sized at 1500 mm x 216 mm, was designed by incorporating series and parallel loops of heating wire with a 1 mm thick Mica sheet placed between the electric heater and the absorber plate. The Mica sheet acts as an insulator between the electric heater and the absorber plate (GI plate). The heat flux can be varied within the range of 0 to 1000 W/m2 using a variac to control the heating process.

The entire setup, extending from the inlet to the orifice plate, is insulated with 25 mm thick polystyrene foam possessing a thermal conductivity of 0.037 W/m- K. The heated plate is a 1 mm thick GI plate with integral rib-roughness on its rear side, serving as the top broad wall of the duct. The bottom wall comprises a 1 mm aluminum plate and 25 mm of wood with insulation underneath. Smooth faced 8 mm thick plywood covers the top sides of the entry and exit sections of the duct.

To determine the mass flow rate of air, a calibrated orifice meter connected to an inclined manometer is employed, with flow control regulated by control valves integrated into the lines. The orifice plate is specifically designed for flow measurement in a pipe with an inner diameter of 53 mm, following the recommendation of Preobrazhensky. It is positioned between flanges to maintain concentricity with the pipe.

The experimental schematic diagram setup that illustrates the test section can be observed, depicting the arrangement of components in the experimental loop. The length of the circular GI pipe utilized is determined by a calculation based on the pipe diameter d1, following the recommendations of Ehlinger, which specify a minimum length of 10 times d1 on the upstream side and 5 times d1 on the downstream side of the orifice plate. In the current experimental setup, a pipe length of 1000 mm (equivalent to 13 d1) is implemented on the upstream side, while a length of 700 mm (equivalent to 9 d1) is used on the downstream side. This configuration ensures optimal positioning of the components for accurate measurements. The calibrated copper-constantan thermocouples, with a diameter of 0.3 mm (24 SWG), are strategically placed at specific locations on the heated wall, as illustrated in Fig. 1, to capture temperature variations effectively. A digital micro voltmeter is integrated into the setup to provide real-time temperature readings from the thermocouples in degrees Celsius, enhancing the efficiency of data collection and analysis.

Moreover, the inclusion of a micro-manometer enables the precise quantification of the pressure drop across the test section, offering valuable insights into the flow dynamics and resistance characteristics of the system. This comprehensive experimental arrangement forms an open flow loop comprising essential components such as the test duct, blower, control valve, orifice plate, and various monitoring instruments for temperature and fluid head. The high accuracy and precision of the thermocouples contribute to reliable temperature measurements, ensuring the consistency of data throughout the experimental procedures. The use of copper-constantan thermocouples further enhances the credibility and stability of the temperature readings obtained during the experiments. The real-time data provided by the digital micro voltmeter facilitates immediate analysis and interpretation of temperature differentials, aiding in the assessment of thermal behaviors within the system.

In conclusion, the experimental setup described above offers a sophisticated and robust platform for investigating the thermal and flow characteristics of the air circulating within the test duct. The integration of advanced instruments and meticulous positioning of components contribute to the accuracy and reliability of the data collected, enabling a comprehensive analysis of the flow behaviors in the system. This experimental configuration not only allows for the precise measurement of temperature differentials but also provides valuable insights into the pressure drop across the test section, enhancing our understanding of the fluid dynamics at play. Overall, this experimental setup represents a significant advancement in the field of fluid mechanics research, offering a wealth of opportunities for in-depth analysis and exploration of flow phenomena.

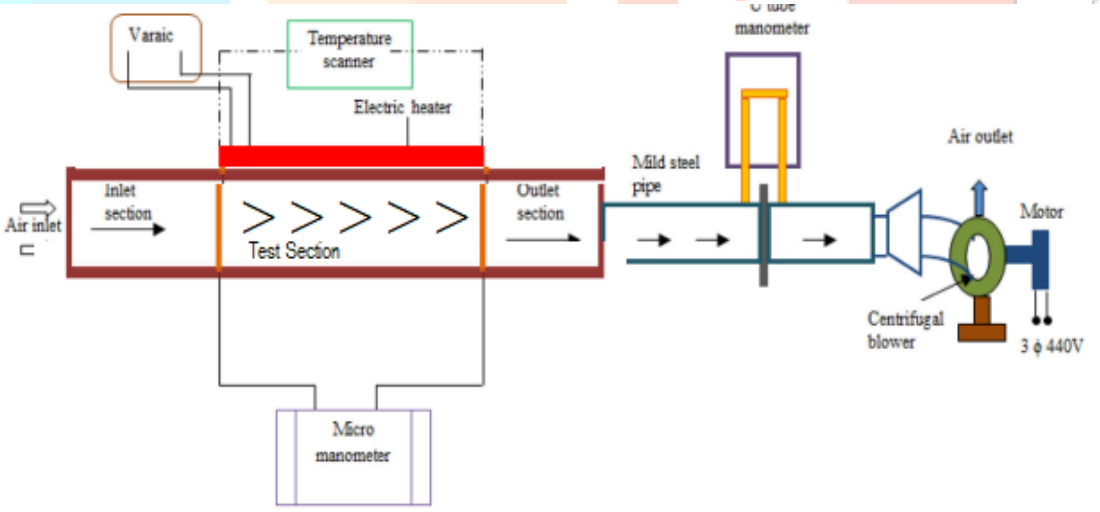

Fig. 1 Schematic Diagram Showing Top View of Experimental Setup

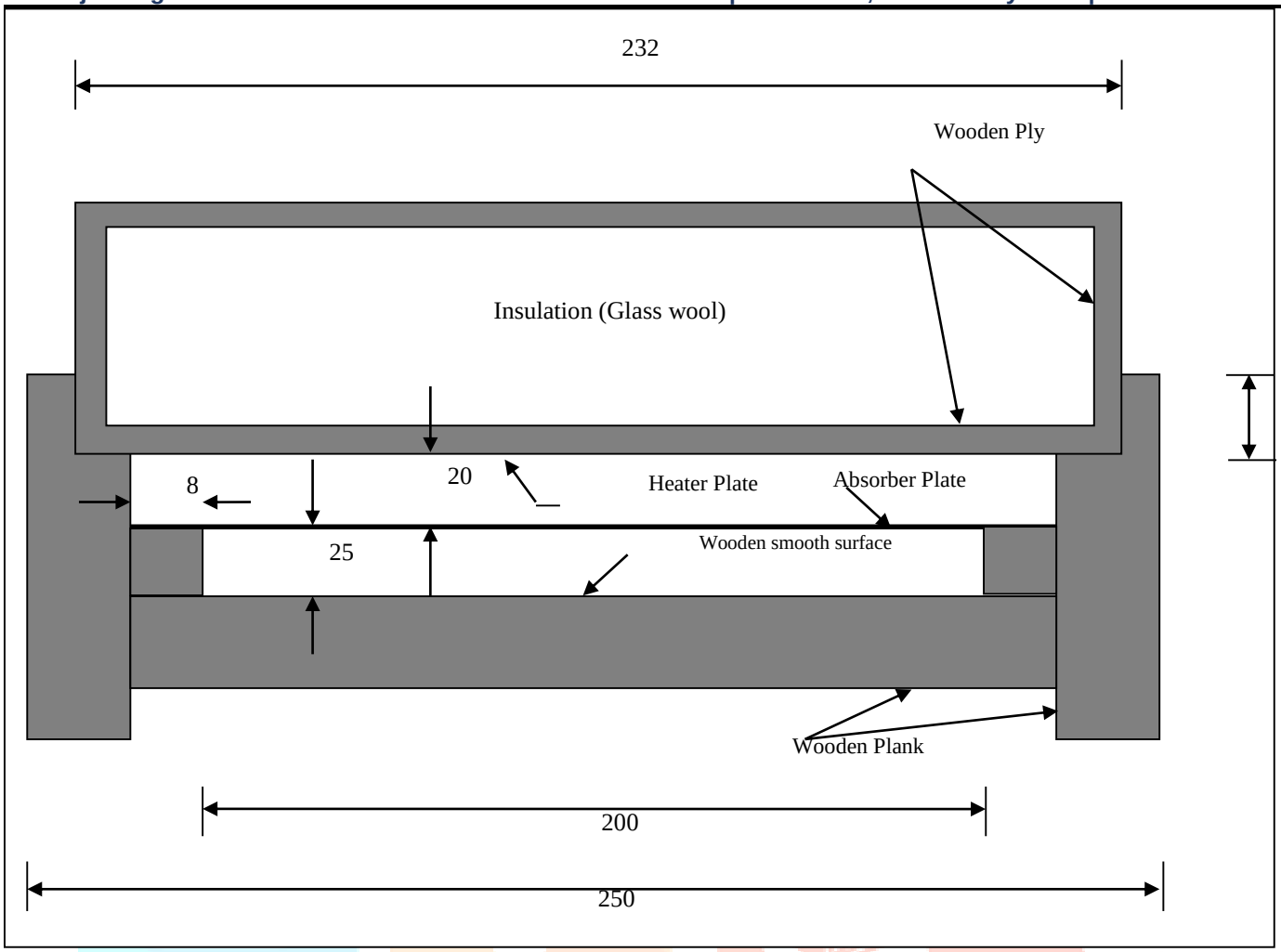

Fig. 2 Cross sectional view of duct

2.1 Roughness Geometry And Range Of Parameters

The system and operating parameters for this study can be found in Table 1. The choice of the relative roughness pitch (p/e) value has been carefully set at 10, in alignment with the optimal value as documented in existing literature. Furthermore, the angle of attack has been specifically designated as 600 to ensure the highest level of heat transfer enhancement is achieved. The configuration of the ribs on the absorber plate has been meticulously illustrated in order to conduct a thorough investigation into their impact on the system. This detailed selection of parameters and setups underscores the precision and rigor with which the experiment has been designed and executed. The deliberate choices made in determining these values and arrangements emphasize the meticulous approach taken in this investigation to gain comprehensive insights into the heat transfer mechanisms at play.

Fig. 3 photo graphic view of absorber plate without gap

Fig.4 photo graphic view of absorber plate with gap

III.VALIDATION OF EXPERIMENTAL SET-UP

In order to assess the validity of the experimental setup, experiments were conducted where all surfaces of the duct were maintained smooth. The outcomes obtained from the smooth duct wall experiments were then juxtaposed with the theoretical results for comparison. The graphical representation in Figure 5 illustrates the changes in the Nusselt number concerning the Reynolds number for the smooth duct. Upon close examination, it is evident that the variance between the experimental outcomes and the theoretical predictions is minimal. This observation highlights a high level of concordance between the theoretical and experimental findings. A similar trend is also evident in the results pertaining to the friction factor, as depicted in Figure 6, reaffirming the strong agreement between the experimental and theoretical data. The consistency between the experimental and

theoretical results across different parameters enhances the confidence in the reliability of the experimental setup and the accuracy of the measurements. This alignment between the two sets of data not only validates the experimental approach but also underscores the robustness of the theoretical framework employed in this study. The findings from these comparisons serve to bolster the overall credibility and robustness of the experimental methodology and the theoretical underpinnings that support it..

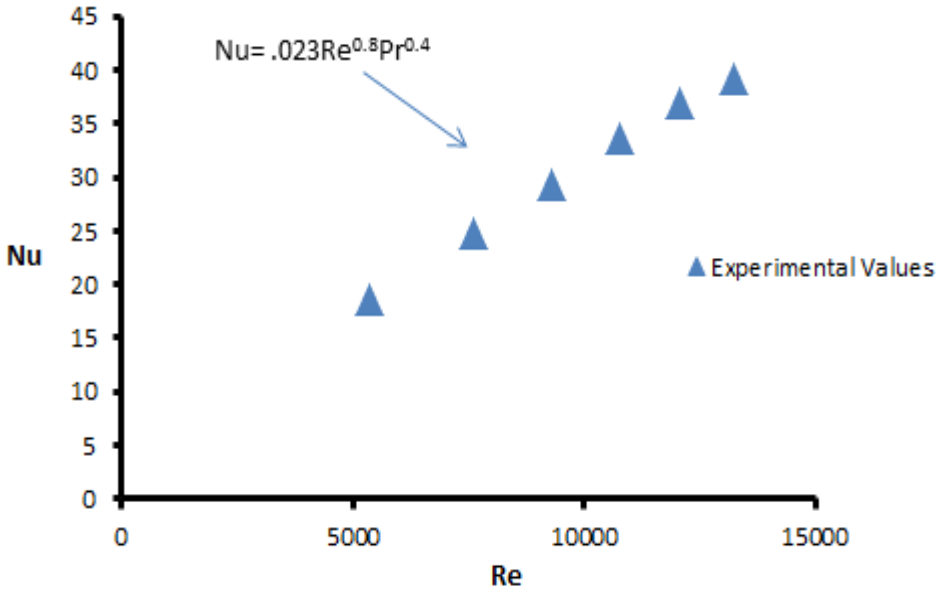

Fig 5. Shows The Variation of Nusselt Number with Reynolds Number

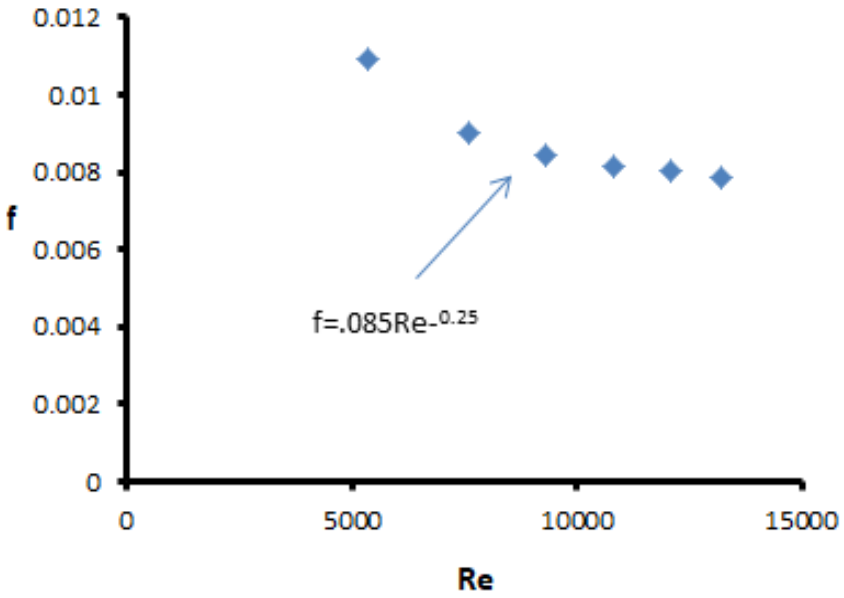

Fig 6. Shows The Variation of Friction Factor with Reynolds Number

IV. RESULTS AND DISCUSSION

The outcomes derived from the conducted experiment have been documented for analysis and interpretation. In Figure 7, the depiction of the correlation between Nusselt number and Reynolds number is presented. Upon scrutiny, it becomes evident that there is a positive relationship between the Nusselt number and the Reynolds number. Specifically, the Nusselt number ranges from 20 to 80 within the Reynolds number span of 5000 to 14000. Notably, the highest Nusselt number value is observed in the case of a rib with a gap roughness configuration. This observation could be attributed to the phenomenon whereby the presence of a gap leads to increased turbulence, thereby augmenting the heat transfer process. This enhancement in heat transfer efficiency is a result of the intensified fluid flow characteristics induced by the presence of the gap, consequently leading to improved thermal performance. The experimental findings underscore the importance of considering surface roughness elements, such as gaps, in enhancing heat transfer rates in practical applications. Moreover, the insights gained from this experiment provide valuable information for the optimization of heat transfer systems in various engineering contexts. It is evident that the manipulation of surface features, such as gaps, can significantly impact the heat transfer characteristics, thereby offering opportunities for improving thermal management strategies in engineering designs.

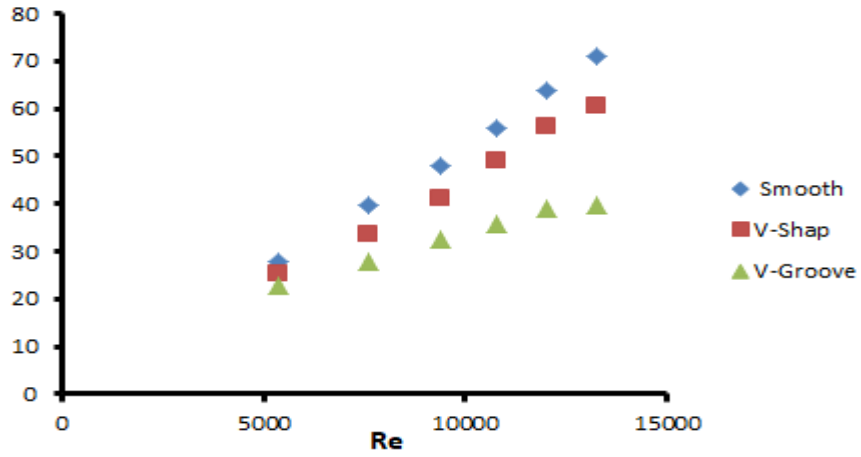

Fig 7 Variation of Nusselt Number with Reynold Numbers

The graphical representation in figure 8 illustrates the relationship between the friction factor and the Reynold number. It can be observed that as the Reynold number increases, there is a corresponding decrease in the value of the friction factor. This phenomenon could potentially be attributed to the reduction in boundary layer thickness as the Reynold number rises, consequently leading to a decrease in the friction factor. Among the various configurations studied, the v-shaped rib with gap roughness arrangement exhibits the highest maximum value for the friction factor, whereas the smooth duct displays the lowest minimum value. Interestingly, the friction factor associated with the v-shaped rib roughness arrangement is notably lower than that of the V-shaped rib with gap configuration. This difference in friction factors highlights the significant impact of surface roughness on the flow characteristics within the duct.

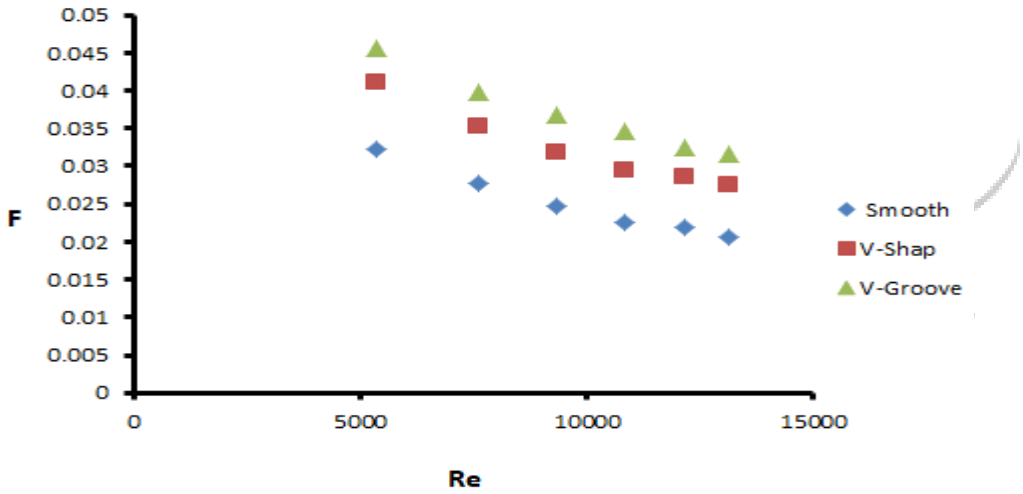

Fig 8 Variation of Friction Factor with Reynolds Numbers

V.CONCLUSION

The current study was carried out with the primary goals of conducting an in-depth examination of v-shaped ribs as a form of artificial roughness, both with and without gaps, on the wide wall of a solar air heater. The experimental setup for analyzing heat transfer and friction factor characteristics was meticulously designed and established for this research. Extensive data was gathered regarding the heat transfer and friction factor attributes of these artificially roughened ducts. A comprehensive analysis was conducted to compare the results obtained from the artificially roughened ducts with those from a smooth duct operating under similar flow conditions, aiming to ascertain differences in heat transfer and friction factor performance. The key findings derived from this investigation are presented in the subsequent sections of this study.

Reynolds Number (Re)	3000 – 15000
Roughness height (e)	1.4mm
Relative roughness height (e/ Dh)	0.030
Relative roughness pitch (p/e)	10
Heat Flux (l)	800W/m2
Angle of attack	600

Channel Aspect ratio (W/H)	8
Test Length	1500mm
Hydraulic Diameter	44.44 m

Table 1: Experimental Conditions

1 The Nusselt number exhibits a positive correlation with the Reynold number, indicating that as the latter increases, the former also increases accordingly. It is noteworthy that the highest Nusselt number value is attained when employing a configuration with v-shaped ribs and gap roughness, due to the presence of v-shaped ribs and gaps inducing a higher degree of turbulence within the flow. This turbulence leads to a significant improvement in heat transfer rates, thereby enhancing the overall heat transfer performance of the system.

2 The decline in the friction factor is directly related to the rise in the Reynold number, showcasing an inverse relationship between the two parameters. It is noteworthy that the friction factor reaches its peak when considering a configuration with v-shaped ribs and gap rib roughness, demonstrating the impact of surface geometry on fluid flow characteristics. Comparatively, the friction factor associated with the v-shaped rib roughness arrangement is lower than that of the v-shaped arrangement with a gap, suggesting variations in flow resistance based on the specific rib configuration utilized. These findings underscore the significance of rib geometry in influencing frictional forces and highlight the need for further exploration in this area of research.

REFERENCES

1. ZVULUN, OFER. (2016). SOLAR AIR HEATER CONSTRUCTION UNIT.
2. ABHISHEK, SAXENA., VARUN., A.A., EL-SEBAII. (2015). A THERMODYNAMIC REVIEW OF SOLAR AIR HEATERS. RENEWABLE & SUSTAINABLE ENERGY REVIEWS, WU, GUOSHENG., PAN, KEXUE. (2014). SOLAR AIR HEATER.
3. DURGESH, KUNVAR, YADAV., AJEET, KUMAR, RAI., VIVEK, SACHAN. (2014). EXPERIMENTAL STUDY OF A SOLAR AIR HEATER.
4. MIROSLAW, ZUKOWSKI. (2016). ASSESSING THE ENVIRONMENTAL IMPACTS OF USING SOLAR AIR HEATERS. ECOLOGY & SAFETY,
5. GUNISETTY, MADHULATHA., M., MOHAN, JAGADEESH, KUMAR., P., SATEESH. (2021). OPTIMIZATION OF TUBE ARRANGEMENT AND PHASE CHANGE MATERIAL FOR ENHANCED PERFORMANCE OF SOLAR AIR HEATER- A NUMERICAL ANALYSIS. JOURNAL OF ENERGY STORAGE, W., SMOLEC., M., JAROSZYŃSKI. (2009). SOLAR AIR HEATER WITH HEAT STORAGE.
6. VIJAY SINGH BISHT RENEWABLE AND SUSTAINABLE ENERGY REVIEWS VOLUME 81, PART 1, JANUARY 2018, PAGES 954-977
7. ARNDT, PAUL, RIIS. (2008). SOLAR AIR HEATER FOR HEATING AIR FLOW.
8. DIBIROV, YAKHYA, ALIEVICH., ALKHASOV, ALIBEK, BASIROVICH., DIBIROV, MAGOMED, GADZHIMAGOMEDOVICH., DIBIROV, KAMIL, YAKHYAEVICH., DIBIROVA, MARZHANAT, MAGOMEDOVNA., ILYASOV, AMIR, MARATOVICH. (2019). SOLAR AIR HEATER.
9. G, N, UZAKOV., S, M, SHOMURATOVA., B, M, TOSHMAMATOV. (2021). STUDY OF A SOLAR AIR HEATER WITH A HEAT EXCHANGER – ACCUMULATOR.
10. ANIL, SINGH, YADAV., TABISH, ALAM., RAJIV, SAXENA., NAVEEN, K., GUPTA., K., VISWANATH, ALLAMRAJU., RAHUL, KUMAR., NEERAJ, SHARMA., ABHISHEK, SHARMA., UTKARSH, KUMAR, PANDEY., YOGESH, AGRAWAL. (2022). A NUMERICAL INVESTIGATION OF AN ARTIFICIALLY ROUGHENED SOLAR AIR HEATER. ENERGIES,
11. DIBIROV, YAKHYA, ALIEVICH., ALKHASOV, ALIBEK, BASIROVICH., DIBIROV, MAGOMED, GADZHIMAGOMEDOVICH., DIBIROV, KAMIL, YAKHYAEVICH., DIBIROVA, MARZHANAT, MAGOMEDOVNA., ILYASOV, AMIR, MARATOVICH. (2019). SOLAR AIR HEATER.
12. R., BAHUGUNA., SUNIL, CHAMOLI., Y, M, BARTHWAL., SUMIT, RANA., ASHUTOSH, GUPTA., VIJAY, SINGH, BISHT. (2022). ECONOMIC ANALYSIS OF ARTIFICIALLY ROUGHENED SOLAR AIR HEATER WITH V-SHAPED RIBS. ACTA INNOVATIONS, DOI: 10.32933/ACTAINNOVATIONS.44.2
13. NEWTON, KUMAR, SINGH., JAYRAM, KUMAR. (2019). SOLAR AIR HEATER DUCT WITH WAVY DELTA WINGLETS: CORRELATION DEVELOPMENT AND PARAMETRIC OPTIMIZATION: A REVIEW.
14. PRADYUMNA, KUMAR, CHOUDHURY., DEBENDRA, CHANDRA, BARUAH. (2017). SOLAR AIR HEATER FOR RESIDENTIAL SPACE HEATING.
15. VIJAY, SINGH, BISHT., ANIL, KUMAR, PATIL., ANIRUDH, GUPTA. (2018). REVIEW AND PERFORMANCE EVALUATION OF ROUGHENED SOLAR AIR HEATERS. RENEWABLE & SUSTAINABLE ENERGY REVIEWS,
16. TEJASWI, JOSYULA., SATYENDER, SINGH., PRASHANT, DHIMAN. (2018). NUMERICAL INVESTIGATION OF A SOLAR AIR HEATER COMPRISING LONGITUDINALLY FINNED ABSORBER PLATE AND THERMAL ENERGY STORAGE SYSTEM. JOURNAL OF RENEWABLE AND SUSTAINABLE ENERGY,
17. AMBREESH, PRASAD, SHUKLA., RAKESH, KUSHWAHA., BHUPENDRA, GUPTA., ANAND, BISEN. (2018). PERFORMANCE ANALYSIS OF SOLAR AIR HEATER USING CFD SIMULATION.
18. ANKUSH, HEDAU., R.P., SAINI. (2023). A REVIEW ON ARTIFICIAL ROUGHENED SOLAR AIR HEATERS WITH AND WITHOUT THERMAL ENERGY STORAGE. INTERNATIONAL JOURNAL OF GREEN ENERGY,
19. SHEETAL, KUMAR, JAIN., GHANSHYAM, DAS, AGRAWAL., ROHIT, MISRA. (2019). A DETAILED REVIEW ON VARIOUS V-SHAPED RIBS ROUGHENED SOLAR AIR HEATER. HEAT AND MASS TRANSFER,

20. Dhananjay, Kumar., Laljee, Prasad. (2020). Experimental Investigation on Thermal Performance in Three-Sided Solar Air Heaters Having an Alignment of Multi-v and Transverse Wire Roughness on the Absorber Plate. Journal of Solar Energy Engineering-transactions of The Asme,
21. Karmveer., N., Kumar, Gupta., Md, Irfanul, Haque, Siddiqui., Dan, Dobrotă., Tabish, Alam., Masood, Ashraf, Ali., Jamel, Orfi. (2022). The Effect of Roughness in Absorbing Materials on Solar Air Heater Performance. Materials,
22. Gabhane, M.G., Kanase-Patil, A.B., Experimental analysis of double flow solar air heater with multiple C shape roughness. Solar Energy 155 (2017) 1411–1416.
23. Gilani, S.E., Al-Kayiem, H.H., Woldemicheal, D.E., Gilani, S.I., Performance enhancement of free convective solar air heater by pin protrusions on the absorber. Solar Energy 151 (2017) 173–185.
24. Pandey, N.K., Bajpai, V.K., Varun, Experimental investigation of heat transfer augmentation using multiple arcs with gap on absorber plate of solar air heater. Solar Energy 134 (2016) 314–326.
25. Karwa, R., Solanki, S. C. and Saini, J. S., "Heat transfer coefficient and friction factor correlation for the transitional flow regime in rib-roughened rectangular duct", Int. Journal of Heat and Mass Transfer, Vol. 42, pp. 1597-1615, 1999.
26. Prasad, B.N., Behura, A.K., Prasad, L., Heat transfer, friction factor and thermal performance of three sides artificially roughened solar air heaters. Solar Energy 130 (2016) 46–59.
27. Behura, A.K., Prasad, B.N., Prasad, L., Fluid flow and heat transfer analysis for heat transfer enhancement in three sided artificially roughened solar air heater. Solar Energy 105 (2014) 27–35.